https://doi.org/10.5194/egusphere-2023-96
Preprint. Discussion started: 21 March 2023

Exploring Non-Gaussian Sea Ice Characteristics via Observing System Simulation Experiments

Christopher Riedel [1] and Jeffrey Anderson [2]

[1]Advance Study Program, National Center for Atmospheric Research, Boulder, Colorado
[2]Data Assimilation Research Section, National Center for Atmospheric Research, Boulder, Colorado

Correspondence: Christopher Riedel (criedel@ucar.edu)

Abstract. The Arctic is warming at a faster rate compared to the globe on average, commonly referred to as Arctic amplification. Sea ice has been linked to Arctic amplification and gathered attention recently due to the decline in summer sea ice extent. Data assimilation (DA) is the act of combining observations with prior forecasts to obtain a more accurate model state. Sea ice poses a unique challenge for DA because sea ice variables have bounded distributions, leading to non-Gaussian distributions. The non-Gaussian nature violates Gaussian assumptions built into DA algorithms. This study configures different observing system simulated experiments (OSSEs) to find the optimal sea ice and snow observation subset for assimilation to produce the most accurate analyses and forecasts. Findings indicate that not assimilating sea ice concentration observations while assimilating snow depth observation produced the best sea ice and snow forecasts. A simplified DA experiment helped demonstrate that the DA solution is biased when assimilating sea ice concentration observations. The biased DA solution is related to the observation error distribution being a truncated normal distribution and the assumed observation likelihood is normal for the DA method. Additional OSSEs show that using a non-parametric DA method does not alleviate the non-Gaussian effects of the sea ice concentration observations, and assimilating sea ice surface temperatures have a positive impact on snow updates. Lastly, it is shown that perturbed sea ice model parameters, used to create additional ensemble spread in the free forecasts, lead to a year-long negative snow volume bias.

1 Introduction

Warming over the Arctic region, a phenomenon commonly referred to as Arctic amplification (Serreze and Francis, 2006), has been identified in both observations (Serreze et al., 2009; England et al., 2021) and climate models (Holland and Bitz, 2003). Numerous studies have found this warming rate to be around twice as fast as the global average (Walsh, 2014; Jansen et al., 2020; Yu et al., 2021). A recent study has found that Arctic amplification-related warming could be three-to-four times faster than the global average, more than double the warming rate previously estimated (Rantanen et al., 2022). Projections of Arctic amplification rely heavily on the ability of coupled numerical models to represent each Earth-system component. One important Earth-system component linked to Arctic amplification–the cryosphere–has gathered attention recently due to the declining summer sea ice extent over the recent decades (Screen and Simmonds, 2010; Jenkins and Dai, 2021). During the winter time, sea ice can act as an insulator trapping ocean heat, created from the absorbed shortwave radiation during the

https://doi.org/10.5194/egusphere-2023-96
Preprint. Discussion started: 21 March 2023

summer sea-ice loss season, within the ocean allowing for cooler winter time atmospheric temperatures (Chung et al., 2021). Additionally, snow cover on top of sea ice can impact seasonal sea ice evolution, growth, and melt (Holland et al., 2021). Providing more accurate sea ice and snow states via data assimilation in our coupled Earth-system modeling frameworks could help improve future projections of the climate and the processes related to Arctic amplification.

Data assimilation (DA) is the action of optimally combining information from prior forecasts with observations to improve the current estimate of the state of any Earth-system component. The statistical methods used to optimally combine this information often have assumptions of gaussianity depending on the choice of the data assimilation method. One data assimilation method that has commonly been applied in Earth-system problems is the ensemble Kalman filter (EnKF; Evensen 2003; Houtekamer and Zhang 2016), which has Gaussian assumptions included in its original Kalman filter formulation (Kalman, 1960). These Gaussian assumptions can lead to biased solutions, when prior forecast distributions are non-Gaussian or errors associated with the observations are also non-Gaussian. Common sea ice variables have both double and single bounded quantities (e.g., double bounded: sea ice concentration; single bounded: sea ice thickness) that lead to non-Gaussian distributions, which would violate Gaussian assumptions. Studies have investigated the performance of different EnKF formulations (stochastic versus deterministic) under non-Gaussian conditions and found that while the stochastic formulation was more stable, both had biased solutions (Lawson and Hansen, 2004; Lei et al., 2010). Different ensemble data assimilation methods that remove the Gaussian assumption have been proposed, however, many have only been tested in low-order models and could be potentially expensive in high-dimensional geophysical models (Pham, 2001; Anderson, 2010; Sakov et al., 2012b; Metref et al., 2014). Here, instead of testing a new ensemble data assimilation method, we will conduct experiments to highlight the impacts the different non-Gaussian sea ice variables can have during the data assimilation updates.

The application of data assimilation to sea ice problems is not a novel idea since this research topic has been investigated for over two decades. Common sea ice descriptive quantities are concentration (e.g., the fraction of a grid cell covered with sea ice) and thickness (e.g., the sea ice surface extending down into the ocean). Previous studies have highlighted the importance of initial conditions when trying to predict Arctic sea ice from the local to seasonal time scales, especially related to accurately initializing sea ice thickness (Msadek et al., 2014; Day et al., 2014; Dirkson et al., 2017). While different data assimilation techniques have been used to update sea ice state variables (Meier and Maslanik, 2003; Van Woert et al., 2004; Lindsay and Zhang, 2006; Stark et al., 2008), numerous studies have tested updating sea ice state variables using the EnKF data assimilation method (Lisæter et al., 2003; Barth et al., 2015). These EnKF studies were tested both in a synthetic observation framework referred to as observing system simulation experiments (OSSEs; Barth et al. 2015; Kimmritz et al. 2018; Zhang et al. 2018) and using real observations from remote sensing platforms (Sakov et al., 2012a; Massonnet et al., 2015). These studies found improvements in both sea ice analyses and their corresponding forecasts related to the spatial sea ice concentration field but little improvement in sea ice thickness. Massonnet et al. (2015) improved the initialization of sea ice cover when updating sea ice thickness via a multivariate framework when assimilating only sea ice concentration observations. More recent studies have tested the assimilation of other sea ice observations (e.g., sea ice thickness) and found further improvements to sea ice states (Mathiot et al., 2012; Chen et al., 2017; Mu et al., 2018; Fiedler et al., 2022). While results from assimilating sea ice thickness observations are positive, they contain large observation uncertainties because satellite remote sensing retrieval algorithms

https://doi.org/10.5194/egusphere-2023-96
Preprint. Discussion started: 21 March 2023

contain large uncertainties due to input parameters and instrument errors (Kwok and Cunningham, 2008; Tilling et al., 2016; Ricker et al., 2017). Further research is needed to determine how to properly handle the uncertainties when assimilating sea ice observations.

This study uses different OSSEs to investigate how the non-Gaussian nature of different sea ice fields impacts the data assimilation-generated sea ice analyses. This study will expand on previous research on sea ice data assimilation that was laid out by Zhang et al. (2018). The OSSEs presented in this study will test different experimental setups to investigate if there is an optimal data assimilation setup for sea ice along with the associated snow cover on top. These experiments will investigate the impacts of post-processing updates for snow on top of sea ice, different assimilated observation combinations, and different data assimilation methods. This study will highlight the impacts of the non-Gaussian nature of certain sea ice variables on the generation of sea ice analyses when using an EnKF data assimilation method. Section 2 describes the sea ice model and the data assimilation experimental setup along with the description of the different OSSEs that were completed. Section 3 presents the results that were found from the different OSSEs. Section 4 discusses conclusions and future work on this research.

2 Methods and Experimental Setup

2.1 DART-CICE data assimilation system

For this study, the Los Alamos Sea Ice Model version 5 (CICE5; Hunke et al. 2015) is used to integrate the analyses forward in time while using an ensemble Kalman filter (EnKF) data assimilation technique to generate analyses. The Data Assimilation Research Testbed (DART; Anderson et al. 2009) software was used to implement the EnKF. Hereafter, we refer to this modeling configuration as CICE-DART. The data assimilation settings follow closely to the optimal settings Zhang et al. (2018) found while the experimental setups will be different.

2.1.1 DART

The data assimilation technique used in this study is the ensemble adjustment Kalman filter (EAKF; Anderson 2001), which is a modified version of the Kalman filter (Kalman, 1960) and a variation of the deterministic ensemble square-root filter (Tippett et al., 2003). The EAKF combines observations with an ensemble of short-term model forecasts over a specific observation window to produce an ensemble of accurate estimate of the sea ice state. One unique aspect of the EAKF is it allows for the use of a flow-dependent background-error covariance, which differs from a static background-error covariance. Additionally, a non-parametric rank histogram filter (RHF, filter option 8 in DART; Anderson 2010) is tested to compare with EAKF results. While the RHF can represent non-Gaussian priors and arbitrary likelihoods for observed variables. Additionally, the RHF can be modified to work with bounded quantities (Anderson, 2020, 2022), however, that application is not applied in this study. To reduce sampling errors due to limited ensemble member size, horizontal localization was applied. A Gaspri-Cohn fifth order polynomial was applied in the horizontal directions to limit observation updates within a specified cutoff radius of 0.05 (i.e., ~320 km; Gaspari and Cohn 1999). Adaptive prior covariance inflation was applied to eliminate potential issues related to

https://doi.org/10.5194/egusphere-2023-96
Preprint. Discussion started: 21 March 2023

poor representation of model errors by “inflating" the prior background fields, increasing the variance by pushing ensemble members away from the ensemble mean (Anderson, 2007). Inflation damping is set to 0.9 to help control the growth of the inflation factor for the different state model variables.

2.1.2 CICE

CICE5 is the sea ice component within the Community Earth System Model (CESM; Danabasoglu et al. 2020) that is used to make projections of the climate. CICE5 simulates the evolution of sea ice and snow as a result of thermodynamic and dynamical processes using a ice thickness distribution. The evolution of sea ice thickness, which is represented by the product of sea ice volume and sea ice area, is accomplished by partitioning the sea ice pack distribution within a grid cell into multiple thickness categories (Lipscomb, 2001). For this study, there are five categories with lower bounds of 0, 0.64, 1.39, 2.47, 4.57 m. Respecting the category bounds provides an unique challenge during the data assimilation step when updating sea ice area and sea ice volume. Snow depth is also partitioned into the five categories. Each thickness category is divided into multiple layers (both sea ice and snow if present) to represent the evolution of sea ice temperature, salinity, and enthalpys related to sea ice and snow. CICE was coupled to a slab ocean model (SOM) that provides the ocean forcing in the form of annually periodic, prescribed ocean forcing data (e.g., sea surface temperatures, ocean heat fluxes). The atmospheric forcing data comes from the Community Atmosphere Model version 6 (CAM6)/Data Assimilation Research Testbed ensemble reanalysis (Raeder et al., 2021) for the time period of interest. Default namelist settings were used in this study (Hunke et al., 2015) except for perturbing several input CICE parameters which will be discussed more in the next section.

2.2 Perfect model OSSEs

Given the uncertainties and potential biases of sea ice thickness and snow-depth observations, this study applies perfect model OSSEs to investigate non-Gaussian impacts. Each ensemble consists of 80 CICE5 members since there are 80 different CAM6/DART reanalysis atmospheric forcing files. Each CICE5 ensemble member uses the same SOM forcing. To increase CICE5 ensemble spread, three different parameters were perturbed that impact albedo, heat transfer through snow and the ability to move sea ice within the ocean. Perturbed parameters are the standard deviation of the dry snow grain radius (R_{snw}), the thermal conductivity of snow (k_{snw}) and the neutral ocean-ice drag coefficient (dragio). These three parameters were chosen because they are among the top parameters to drive variability within CICE5 in both summer and winter (Urrego-Blanco et al., 2016). To reach a spun-up equilibrium sea ice and snow state, a single member is run for 40 years using periodic atmospheric forcing for year 2012. To build our 80 member ensemble, we first used only the 80 different atmospheric forcings to cycle over 2012 for 10 years to build in variability related to the atmosphere. Then, each member is run for an additional 15 years, cycling over 2012, using the distinct atmospheric forcing and parameter set to generate free forecasts that can be used as a reference case (Fig. 1). One of the free forecast members is chosen as the simulated “truth." For this study, the free forecast ensemble mean is negatively biased compared to the truth member for the different sea ice and snow characteristics. The free forecasts will provide a reference for comparison with the different data assimilation experiments.

https://doi.org/10.5194/egusphere-2023-96
Preprint. Discussion started: 21 March 2023

Since satellites can not retrieve the multi-category model quantities, aggregate synthetic observations are generated from the truth member to produce sea ice concentration (SIC), sea ice thickness (SIT), snow depth (SNWD), and sea ice surface temperature (SIST). SIC is just the sum of the concentration values in the different thickness categories. SIT is computed by summing the sea ice volumes in the different thickness categories than dividing by the aggregated sea ice concentration. SNWD is computed in the same fashion as SIT except using summed snow volumes. SIST is the concentration weighted mean temperature across the different thickness categories on the surface of the sea ice. Normally, synthetic observations are created by adding a draw from a normal distribution with zero mean and specified observation error standard deviation. This method can be used to create synthetic sea ice surface temperatures. However, sea ice and snow quantities have both single (SIT, SNWD) and double (SIC) bounds in their representation. Because of this, we will use a single (SIT,SNWD) and double (SIC) truncated normal distribution when generating the synthetic observations. The observation error standard deviation, which follows those found in Zhang et al. (2018), is 15% of the true values of SIC and 0.1 m for SIT. The observation error standard deviation is 10% of the true values of SNWD (Rostosky et al., 2020) and 1.5°C for SIST (Hall et al., 2015). The locations for all synthetic observation types were based on 10-second CryoSat-2 locations, which provides a realistic observational network for testing (Fig. 2). The multi-category model variables that are updated via the data assimilation or post-processing are AICEN, VICEN, and VSNON, which represent sea ice concentration, sea ice volume, and snow volume. When those multi-category model variables are summed up over the different categories, they are referred to as SIC, VICE, and VSNO.

Six different experiments were completed to test different observation combinations, data assimilation techniques, and post-processing updates (Table 1). Experiment 1 is an extension of the work completed by Zhang et al. (2018) where they only allowed observation increments to update the sea ice area in the different categories while updating the sea ice snow volume via post-processing. In experiment 1, we allow sea ice concentration and volume to be updated by SIC and SIT observations while updating snow volume via post-processing. The equation for post-processing snow volume (VSNON) updates in the different categories is the following:

$$\mathrm{VSNON}^{\mathrm{posterior}} = \mathrm{AICEN}^{\mathrm{posterior}} \times \mathrm{hsnon}^{\mathrm{prior}}, \tag{1}$$

where AICEN is the sea ice concentration in the different categories and hsnon are the category-based snow thickness. In experiment 2, the post-processing snow volume updates are removed and assimilation of SNWD is included in the observation subset. To test the non-Gaussian effects of SIC observations, experiment 3 only assimilates SIT and SNWD while allowing the sea ice concentration, sea ice volume and snow volume state variables to be updated from the observation increments. Experiment 4 investigates the impacts of using a non-parametric data assimilation method, the rank histogram filter, when working with the non-Gaussian sea ice and snow variables in the CICE model. Experiment 5 investigates the impacts of having sea ice thickness and snow depth output from CICE instead of having the forward operators within DART compute these quantities. This arises from the fact that prior inflation is applied, which can push either the sea ice concentration or volume below the zero bound. Since computing sea ice thickness or snow depth is the division of either sea ice or snow volume by the sea ice area, this could lead to shuffling of the distribution if values become negative. Lastly, experiment 6 tests the impacts of assimilating additional SIST observations to further improve the updates of sea ice states along with snow states.

https://doi.org/10.5194/egusphere-2023-96
Preprint. Discussion started: 21 March 2023

Due to the bounds related to sea ice and snow state variables, there are different conditions when special treatment is needed to ensure the respected bounds are met. SIC (summed sea ice concentration across the categories) must remain between 0 and 1. Similarly, sea ice and snow volumes (summed across the categories) must remain above zero. If negative values occur for SIC or the volumes, all categories are set to zero. Additionally, category-based sea ice concentration values are scaled if the SIC exceeds one after the assimilation updates. In the event SIC exceeds one the scaling of the category-based sea ice concentration is as follow:

$$\begin{aligned} \text{squeeze} &= \frac{1.0}{\text{SIC}}, \\ \text{AICEN} &= \text{AICEN} * \text{squeeze}, \end{aligned} \tag{2}$$

where squeeze is the factor by which the individual category-based AICEN values are adjusted. In the case where SIC is within the bounds but individual categories become negative, those categories are set to zero and the remaining non-zero categories are reduced proportionally to compensate for the negative amount. Lastly, special care is taken to account for the cases where SIC is greater than zero but sea ice volume become zero due to the assimilation updates. A new sea ice volume is computed for the category, to replace the zero value, by multiplying the mid-point sea ice thickness by the sea ice concentration for the associated category.

The same initial conditions used to generate the free forecasts were used for the experiments listed in Table 1. The free forecasts provide a reference to the amount of variability that was generated during the spin-up process (Fig. 1). All experiments were initialized on 1 January 2013 and the cycling period was for the entire year 2013. In all experiments, observations are assimilated at a daily interval.

2.3 Model Verification Metrics

Total sea ice area, sea ice volume and snow volume will be forecast quantities used to evaluate CICE-DART performance over the cycling period. The bias of the forecast quantities is defined as the ensemble mean minus the truth and will be calculated daily. Total sea ice area was chosen as it provides the actual area covered by sea ice compared to the common Arctic sea ice extent is the total area where the sea ice concentration exceeds 15%. Total sea ice area will allow for better evaluation of the actual sea ice concentration values since they are used in the calculation compared to sea ice extent. Additionally, mean spatial biases will be computed for SIC, sea ice volume and snow volume over different cycling periods. Welch's t-test will be applied to test for significant biases (Welch, 1947).

Mean absolute bias (MAB) and mean square error (MSE) will be computed for total sea ice area, sea ice volume and snow volume for additional performance evaluation. The integrated ice-edge error (IIEE) is another forecast metric that will be applied to evaluate sea ice coverage in this study (Goessling et al., 2016). IIEE will evaluate potential sea ice edge differences between the ensemble mean and the truth. IIEE is more suitable for user forecast evaluation of the sea ice edge compared to the traditional sea ice extent (Tietsche et al., 2014). The IIEE is the sum of the area grid boxes where the ensemble mean and the truth disagree on whether sea ice is present (over-prediction) or not (under-prediction). Like in previous studies computing IIEE, a SIC threshold of 15% is used to determine whether a grid cell is identified as having sea ice (Goessling and Jung,

https://doi.org/10.5194/egusphere-2023-96
Preprint. Discussion started: 21 March 2023

2018; Zampieri et al., 2018). An attractive feature of IIEE is that it can be decomposed into an absolute extent error (AEE) and a misplacement error (ME). AEE is the absolute difference (|over-prediction - under-prediction|) between predictions, which can help determine whether there is a bias for over or under predicting sea ice coverage. MEE is the misplacement error (2 $\times$ **min**(over-prediction,under-prediction)) reflecting whether there is too much sea ice in one location and too little in another. IIEE along with AEE and ME will be computed daily. A Welch's t-test was used to determine whether there were significant differences between MAB, MSE, and IIEE values between experiments. Lastly, Spearman correlations are computed between the perturbed parameters and different CICE model output.

3 Results and discussion

3.1 Optimization of sea ice and snow data assimilation

In experiments 1–3 investigate which assimilated observation subset produces the most accurate forecasts for both sea ice and snow. Daily biases of total sea ice area, sea ice volume and snow volume are computed throughout the cycling period to compare the performance of the experiments with the truth and free forecasts (Fig. 3). For experiment 1, SIC and SIT observations are assimilated which provides updates to the prognostic sea ice state variables (AICEN and VICEN) while the prognostic snow state variable (VSNON) is updated via post-processing. Compared to the free forecast, experiment 1 performs better for both total sea ice area and sea ice volume. However, total sea ice area and sea ice volume were negatively biased from the start of the melt season in May until the re-freeze in September. Total snow volume for experiment 1 is comparable to the free forecasts. This means the post-processing updates for the snow state variable are not as accurate compared to the sea ice state variables, which are updated directly from the multivariate data assimilation step. Experiment 2 assimilates snow depth observations so no post-processing is performed for snow. While there is little impact on biases associated with the sea ice quantities, the biases are reduced for total snow volume throughout the cycling period with smaller bias than the free forecast. Experiment 3 removed SIC as an assimilated observation, which leaves only SIT and SNWD observations that are assimilated. For sea ice area and sea ice volume, the negative biases during the summer are near zero. Improvements in total snow volume for experiment 3 are isolated to the start of the melt season, however, the biases are similar to the other experiments after this period. Regardless of these improvements, total snow volume is negatively biased throughout the entire cycling period for experiments where SNWD observations are assimilated. Removing SIC observations from the assimilated observation subset eliminates a non-Gaussian component during the assimilation step, which could be the driving factor for the poor forecasts in experiments 1 and 2.

Temporal forecast metrics are computed over the cycling period to pin-point which experiment is more accurate (Fig. 4). Experiments 1 and 2 have the lowest total IIEE and are significantly different from the free forecast and experiment 3. This means that experiments 1 and 2 provide a more accurate sea ice coverage over the cycling period. This might seem inconsistent since experiment 3 daily biases were smaller. Sea ice area MSE and MAB for experiment 3 are lower and significantly different than the other experiments and the free forecast. This means removing the SIC observations provided a more accurate forecast of the sea ice area, however, this did have a negative impact on predicting the sea ice edge in experiment 3. This indicates

https://doi.org/10.5194/egusphere-2023-96
Preprint. Discussion started: 21 March 2023

that the SIC observations play an important role in maintaining the sea ice edge close to the truth. Additionally, all experiments perform better for sea ice volume compared to the free forecast, with experiment 3 being the most accurate. For snow volume, experiment 1 is not statistically better than the free forecast, meaning post-processing snow updates is not an optimal method. Once again, experiment 3 performs the best for snow volume even though SIC observations are not assimilated. While not assimilating SIC observations improves most forecast metrics, it is obvious that these observations should be crucial for representing the sea ice edge accurately.

While experiment 3 provided the most accurate forecasts for the aggregated quantities, like total sea ice area, it is unclear where those improvements occurred spatially over the Arctic at the start of the melt season. To gain more insight on the improved results from experiment 3, May-through-June averaged spatial biases of SIC, VICE and VSNO are computed for the free forecast and each experiment (Fig. 5). For SIC, there are significant biases for the free forecast where the SIC values are too large over the central Arctic and too small near the sea ice marginal zone. Experiments 1 and 2 show predominantly significant negative biases over the sea ice for SIC while experiment 3 has reduced the spatial biases to near zero. The negative SIC spatial bias over the central Arctic explains why the total sea ice area for experiments 1 and 2 performed poorly compared to experiment 3. However, there are areas of larger bias value near the sea ice margin for experiment 3 where it was less accurate representing the sea ice edge, according to total IIEE. While all experiments reduced the magnitude of the VICE spatial bias, there is still an overall significant negative bias for experiments 1 and 2. The spatial biases for experiment 3 are near zero and there are essentially no areas of significant bias. For VSNO, there is a big difference between the spatial biases for experiments 1 and 2, highlighting the benefits of assimilating SNWD observation over post-processing VSNO updates. In experiment 3, there is an overall reduction in the significant negative biases over the central Arctic compared to experiment 2. In experiments 1 and 2, the SIC observations have a negative impact on both the observed and non-observed model state variables. Removing SIC observations from the assimilated observation subset reduced the spatial coverage of significant biases for all state model variables.

An analysis increment (AI) indicates how the observations are pushing or pulling state model variables. Evaluating AIs will help determine how the SIC observations impact the different data assimilation experiments. For experiment 3, there is a reduction in the magnitude of the spatial AIs at the start of the melt season compared with experiments 1 and 2 (Fig. 6A). The AI reduction is mainly located over the central part of the Arctic, where SIC values for all ensemble members are close to 1. This means the assimilation of the SIC observations leads to low biased SIC analyses. The SIC AIs become more similar across the experiments as one moves away from the central Arctic toward the sea ice marginal zone. The AI patterns and magnitudes near the sea ice edge for experiment 3 are different than one might expect due to the increase in IIEE. However, these AIs are averaged from May through June, so the IIEE might be picking up on sea ice edge errors at different times throughout the cycling period. It is a similar story for the VICE, where there is a reduction in the AI magnitude over the central Arctic for experiment 3 compared to experiments 1 and 2 (Fig. 6B). For VSNO AIs, there is a flip in the sign between experiments 1 and 2 (Fig. 6). The negative VSNO AIs in experiment 1 are connected to the SIC AIs due to the equation for the post-processing (Equation 1). Since SIC AIs are mainly negative over the central Arctic, this would also lead to negative VSNO AIs over this region due to the post-processing method. The differences in VSNO AIs between experiments 2 and 3 are small, meaning

https://doi.org/10.5194/egusphere-2023-96
Preprint. Discussion started: 21 March 2023

that the removal of SIC observations from the assimilated subset does not have a negative impact on the adjustments. Overall, experiment 3 provides the optimal setup for sea ice and snow data assimilation. Even with a slightly higher IIEE, the removal of the SIC observations from the assimilate observation subset did provide better results. Further investigation is needed to understand the reason behind the persistent negatively biased total snow volume compared to the truth.

3.2 Simplified Data Assimilation Experiment

To further investigate the poor results when assimilating SIC observations, a simplified data assimilation experiment is setup. This simplified DA experiment will mimic SIC during the wintertime over the pole, meaning the truth SIC does not change over time. With a constant truth value that does not change, observations are created that will be assimilated over the cycling period. The truth SIC value is 0.99 and it's corresponding observation error uses the same method as the OSSE experiments. Two different initial ensemble distributions are created; small ensemble spread (standard deviation: 0.0007) and large ensemble spread (standard deviation: 0.0142). When prior inflation is tested, it will be set to a constant inflation factor set of 2. All other data assimilation settings (e.g., filter type EAKF) are the same as those in the experiments. Four mini experiments are completed using a combination of the different initial ensemble spreads and prior inflation either turned off or on. The experiments are cycled 5,000 times, assimilating the observations generated from the truth using a truncated normal distribution. These experiments will work with SIC directly, meaning there are no thickness categories as in CICE. This means that the mapping between observation space to state space is linear, further simplifying this data assimilation experiment.

For all experiments, the prior ensemble mean drifts away from the true value and moves toward the average observation value over the cycling period (Fig. 7). The rate at which the prior ensemble mean moves toward the average observation value depends on both the initial ensemble spread and if prior inflation is applied. For small initial ensemble spread, the prior ensemble mean drifts away from the true value faster with prior inflation compared to when prior inflation is turned off (Fig. 7A, B). While it takes many cycling times, the prior ensemble mean is pulled below the true value without prior inflation for a small initial ensemble spread. When the initial ensemble spread is increased, the prior ensemble mean moves away from the truth at an increased rate with and without prior inflation (Fig. 7C, D). This effect is similar to the results in experiment 2 related to total sea ice area. During the wintertime, SIC ensemble variance is small over most of the ice pack, which is why data assimilation has little impact (similar to results in Fig. 7A). However, once the melt season starts, there is an increase in the SIC variance. Combining the increased SIC variance with prior inflation likely leads to a negatively biased solution in experiment 2 (Fig. 3A).

The fact that the prior ensemble mean moves away from the true value regardless of the initial ensemble variance demonstrates that our data assimilation solution is biased. This is due to the fact that our observation error distribution is a truncated normal while the observation likelihood for the EAKF is assumed to be normal. Applying a non-Gaussian distribution for observation errors while using a Gaussian observation likelihood can lead to erroneous observation impacts, biasing analysis estimates (Pires et al., 2010; Fowler and Jan Van Leeuwen, 2013). The effects of prior inflation exacerbate the bias by increasing prior variance, which weights the observations even more. A better choice might be an optimal combination of distributions representing the prior state and the observation errors more appropriately, as laid out in Anderson (2022).

https://doi.org/10.5194/egusphere-2023-96
Preprint. Discussion started: 21 March 2023

3.3 Further discussion on sea ice data assimilation

The removal of SIC as an assimilated observation improved forecasts of total sea ice, however, forecasts of the sea ice edge were less accurate according to the total IIEE. This suggests that, near the sea ice margin, there are benefits to assimilating SIC observations and that SIT observations provide poor multivariate updates for AICEN. Three additional experiments were completed to investigate the sea ice impacts when using a non-parametric RHF, modified forward operators for thickness observations, and assimilation of SISTs. Each additional experiment is compared with experiment 3. Experiment 4 performs worse than experiment 3 during the summer according to daily biases of total sea ice area, sea ice volume and snow volume (Fig. 8). The use of the non-parametric RHF in experiment 4 did not handle the SIC observations better. Compared to experiment 3, experiments 5 and 6 have similar daily biases for total sea ice volume and snow volume, however, not for total sea ice area. Experiments 5 and 6 have persistent, larger daily biases during the summer compared to experiment 3. There does appear to be a slight improvement in total snow volume for experiment 6 compared to compared experiment 3 during May, however, there are still negative biases throughout the cycling period.

Experiment 4 does the best job representing sea ice coverage since its total IIEE is the lowest and it is significantly different from the other experiments (Fig. 9). Experiment 4 assimilates SIC observations, which is likely why it is similar to our previous result from experiment 2 (compare Fig. 4A with Fig. 9A). Experiments 5 and 6 essentially have the same total IIEE, which are statistically worse than experiment 3. The modification to the forward operator along with assimilating SIST observations poorly represents sea ice coverage. For total sea ice area and sea ice volume, experiment 4 has the largest aggregated errors that are significantly different from the other experiments (Fig 9B, C). This result is similar to experiment 2, where SIC observations were assimilated. Experiment 3 does the best job representing the total sea ice area and sea ice volume. However, one thing that needs to be mentioned is that experiment 6 uses the modified forward operator. Since the sea ice statistics appear very similar between experiments 5 and 6, the modified forward operator could be the reason why the results for experiment 6 are worse than those for experiment 3.

Evaluating SIC over the start of the melt season (May-through-June) reveals that experiment 4 has mostly significant negative biases compared to the truth (Fig. 10A). This result is similar to experiment 2, where the EAKF is used instead of the RHF. Compared to experiment 3, there are larger, positive SIC biases for experiments 5 and 6 near the sea ice margin. These biased areas are mainly located in the Baffin Bay, Greenland Sea and Barents Sea. The poor representation of the sea ice margin zone for experiments 5 and 6 could explain the larger total IIEE compared to experiment 3. Experiment 4 has significant negative sea ice volume biases over most of the sea ice pack (Fig. 10B). Again, this agrees with the spatial biases for experiment 2 over this period, further showing that switching to the RHF over the EAKF did not help alleviate the impacts of the SIC observations. The spatial biases of sea ice volume for experiments 5 and 6 closely resemble those found in experiment 3, except near the sea ice margin. The modified forward operator might introduce poor sea ice margin updates without the constraint of the SIC observations in this region. Overall, switching the data assimilation filter type did not fix the issues related to assimilating SIC observations and there are potential issues with using the modified forward operator near the sea ice margin. However,

https://doi.org/10.5194/egusphere-2023-96
Preprint. Discussion started: 21 March 2023

the spatial biases are similar over most of the central Arctic meaning more investigating is needed to determine the negative impacts of the modified forward operator.

3.4 Further discussion on snow data assimilation

Regardless of the experiment, the daily biases for snow volume are negative throughout much of the entire cycling period compared to the truth (Figs. 3C). Even the daily biases for the additional experiments are mainly negative throughout the cycling period (Fig. 8C). The use of the RHF in experiment 4 does not improve the representation of snow volume, while experiments 5 and 6 are similar to experiment 3. For snow volume, experiment 6 is performing better than experiment 3 throughout May. Experiment 6 has smaller MSE and MAB values for snow volume and is significantly different from experiment 3 (Fig. 9C). This means assimilating additional SIST observations provided a more accurate update to snow volume. While mainly negative, the magnitude of the spatial biases are larger with more areas with significant biases for experiment 4 (Fig. 10C). Even though experiment 6 had the lowest MSE and MAB for snow volume, it is hard to identify any particular spatial region over the sea ice where the biases are closer to zero compared to the other experiments (Fig. 10C).

Further investigation is needed to fully understand why the snow volume is negatively biased regardless of the experimental setup. Experiment 3 will be further evaluated to investigate the reason for the low bias in snow volume. Since the ocean forcing is the same across ensemble members, the atmospheric forcing is evaluated for the ensemble mean. Breaking down the individual atmospheric heat fluxes, the shortwave radiation has the largest bias compared to the truth (Fig. 11A). The other atmospheric heat fluxes have smaller and near zero biases for most of the cycling period. The positive shortwave heat flux bias occurs during sunrise over the Arctic, which also corresponds to the period in experiment 3 where the daily biases for snow volume are the largest (Fig. 3C). The spread in the absorbed shortwave heat flux grows during the onset into summer, which is during the start of the melt season for snow (Fig. 11B). The ensemble on average has absorbed too much incoming shortwave radiation compared to the truth. Interestingly, the spread of the absorbed shortwave heat flux collapses at the start of July, when the snow on top of the sea ice would be at it's minimum (Fig. 3C). One feature that can impact absorbed shortwave radiation and is connected to snow would be surface albedo (Fig. 11C). During the same period, the spread in absorbed shortwave heat flux increases and there is an increase in the surface albedo spread. The spread in the surface albedo then collapses, like the incoming shortwave radiation heat flux, near the start of July. The surface albedo is on average too small compared to the truth, which could be the reason for the positive bias in the absorbed shortwave radiation. Lastly, the ensemble members almost appear sorted, for both absorbed shortwave radiation and mean surface albedo, hinting that there is something systematic driving these quantities.

One potential reason that could be driving the negative biases found for the ensemble mean snow volume is the snowfall originating from the atmospheric forcing file for the truth member is an outlier. This does not appear to be the case when comparing daily biases of snowfall for the ensemble mean (Fig. 11D). The snowfall biases for the ensemble mean are near zero and fluctuate about the zero line, meaning there is no clear systematic difference from the truth. One issue that has not been discussed is the role the CICE perturbed parameters could be playing in the snow evolution. Perturbed parameters have been used over the years to create more spread in atmospheric models (Murphy et al., 2004; Stainforth et al., 2005; Christensen

https://doi.org/10.5194/egusphere-2023-96
Preprint. Discussion started: 21 March 2023

et al., 2015; Orth et al., 2016), where the system is more chaotic. However, the impact the perturbed parameters would have on a less-chaotic system like the cryosphere is unclear. Concerning total snow volume, there are larger and more significant correlations between the R_{snw} parameter compared to the other perturbed parameters throughout the cycling period (Fig. 12A). The positive correlations mean that larger standard deviations of dry snow grain radius lead to more total snow volume. This connection is a result of the larger standard deviations of dry snow grain radius resulting in a higher albedo, reflecting more incoming shortwave radiation (Hunke et al., 2015). Looking at snow melt, there are negative and significant correlations during the melt season for the R_{snw} parameter, while the other parameters have little significant correlations (Fig. 12B). This means there is more snow melt for lower standard deviations of dry snow grain radius, resulting in more absorbed shortwave radiation due to a lower surface albedo. The R_{snw} parameter for the truth member is located above the 75th percentile compared with the rest of the perturbed R_{snw} parameters (Fig. 12C). Even with snow assimilation updates, the impact from the perturbed R_{snw} parameter might play a larger role in snow evolution. Due to this fact, it is not surprising to find that the ensemble mean is negatively biased compared to the truth for total snow volume.

4 Conclusions

To advance our understanding of the global climate, it is critical to improve our representation of the different underlying Earth-system components within our coupled numerical climate models. One important Earth-system component–the cryosphere–has gathered recent attention due to declining Arctic summer sea ice and the link back to Arctic amplification. Data assimilation methods, like the ensemble Kalman filter (EnKF), are one way to improve the representation of sea ice states by exploiting information from observations taken from satellites. However, the formulation of the EnKF has Gaussian assumptions and most state variables representing sea ice have some form of boundedness, which can lead to non-Gaussian distributions near those bounds. This study investigates the data assimilation impacts of the non-Gaussian nature of sea ice and snow variables on the generation of analyses within different observing system simulation experiments (OSSEs). The different OSSEs presented in this study will test for the optimal setup for sea ice and snow data assimilation when dealing with non-Gaussian states.

In this study, a sea ice model called CICE is coupled to the ensemble data assimilation software provided by DART to obtain a sea ice modeling system called CICE-DART. CICE-DART is used to conduct OSSEs to test different data assimilation configurations. Six different experiments were completed to test different observation combinations, data assimilation techniques, and post-processing updates (Table 1).

Experiments 1–3 explore the impacts different assimilated observation subsets have on generating the most accurate forecasts for both sea ice and snow states. According to the daily biases and aggregated statistics, experiment 3 is more accurate, when compared to the truth, for sea ice area, sea ice volume, and snow volume. This highlights the negative impacts that SIC observations have on forecasts when they are assimilated in experiments 1 and 2. Doubly bounded SIC observations can impose non-Gaussian effects on both during the summer and winter. Early springtime SIC truth values are still close to one, maximizing their observation error (15% of the truth value), which leads to observations being drawn further below the truth due to the bound at one. Additionally, prior spread increases both due to the start of springtime melt and prior inflation.

https://doi.org/10.5194/egusphere-2023-96
Preprint. Discussion started: 21 March 2023

Combining the low biased observations with the increase in prior spread leads to an enhancement of the non-Gaussian effects during the early springtime. Interestingly, SIC observations do provide positive updates in the sea ice margin, shown by total IIEE being lower in experiments 1 and 2. Due to positive updates in the sea ice margin, it would be optimal to assimilate SIC observations within the data assimilation system.

To better understand the assimilation impacts due to the SIC observations, a simplified data assimilation experiment is completed. This simplified experiment mimics central Arctic SIC during the winter time, meaning the truth does not change. The generation and assimilation of SIC observations followed the same setup as the CICE-DART experiments. In each simplified experiment, the prior ensemble mean moves away from the truth and closer to the average observation value during the cycling period. The rate at which the prior ensemble mean moved away from the truth depended on the initial ensemble size and whether prior inflation was used. These experiments verified that near a bound, the performance of the EAKF is suboptimal. We believe the suboptimal performance is linked back to using a truncated normal distribution as the observation error distribution while the observation likelihood for the EAKF is assumed to be normal. Future projects focusing on sea ice data assimilation might want to consider a different choice for the observation likelihood specification, similar to those laid out in Anderson (2022).

Additional OSSEs are performed to further investigate potential data assimilation improvements for sea ice (Table 1). A non-parametric RHF was tested since it was developed for non-Gaussian situations. The results showed little improvement over the EAKF when assimilating SIC observations. This is likely linked back to the RHF making some non-parametric assumptions on the tails and an assumed normal likelihood when the distribution is not bounded. :The modification to the forward operators did not improve the sea ice data assimilation, especially related regarding sea ice edge errors. This could mean that there are few instances of shuffling the sea ice thickness distribution due to the prior inflation. Additionally, the multivariate update between sea ice thickness observations and sea ice area might be the reason for the increase in sea ice edge errors. Lastly, assimilating SISTs did not lead to increased skill for sea ice variables. The correction between the SISTs and sea ice model variables might not be significant, leading to little improvement.

Evaluation of the additional OSSEs are performed to investigate their impact on snow updates. The improvements associated with using the non-parametric RHF over the EAKF were small for snow volume. This means that the non-Gaussian impacts from the SIC observations were negative on snow volume updates. Additionally, the modified forward operators have little impact on snow volume updates. However, there is a slight improvement in the snow volume when SISTs are assimilated. This improvement occurred during May and not over a specific area of the sea ice. This could mean the connections between SISTs and snow are more significant than compared to sea ice, where the impacts were less impactful. Regardless, all additional experiments still experienced a negative bias throughout the entire cycling period. Further investigation revealed that one of the perturbed parameters could be driving the negative bias for snow volume. Correlations were larger and significant between snow variables and the representation of the dry snow grain radius size (R_{snw}) within our ensemble. Due to the random choice of the R_{snw} parameter for the truth member, it is likely the reason the ensemble mean is negatively biased for snow volume.

Future work will further investigate how to properly assimilate SIC observations. Due to their positive impact on the sea ice margin zone, an experiment could be proposed where only SIC observations are assimilated in that remote location. Addi-

https://doi.org/10.5194/egusphere-2023-96
Preprint. Discussion started: 21 March 2023

tionally, further investigation is needed to test the use of more sophisticated data assimilation methods that accurately handle non-Gaussian distributions. Lastly, supplementary OSSE experiments could be completed with a different ensemble member chosen as the truth to further understand the impacts the perturbed parameters have on representing snow volume. These additional experiments would further help us understand the optimal data assimilation setup for representing sea ice and snow in climate analyses.

Code availability. CICE version 5 used for the experiments described here is part of the CESM2 framework which is publicly available for download from https://www.cesm.ucar.edu/models/cesm2/download.html (accessed in August of 2020). The data assimilation software used here can be downloaded from https://github.com/NCAR/DART (accessed in August of 2020).

Data availability. Post-processed and raw data from the experiments described here are stored on NCAR's campaign storage.

Author contributions. The development of the CICE-DART framework was completed by both CR and JA. CR prepared and performed the experiments under the supervision of JA. The manuscript was composed by CR with contributions and feedback from JA.

Competing interests. The contact author has declared that neither they nor their co-author have any competing interests.

Acknowledgements. This material is based upon work supported by the National Center for Atmospheric Research, which is a major facility sponsored by the National Science Foundation under Cooperative Agreement No. 1755088. Special thanks to the entire DART team for providing helpful input and source code support. I would also like to thank Cecilia Bitz and Molly Wieringa for their fruitful discussions. We thank the editor and anonymous reviewers for constructive comments that helped improve the manuscript.

https://doi.org/10.5194/egusphere-2023-96
Preprint. Discussion started: 21 March 2023

References

Anderson, J., Hoar, T., Raeder, K., Liu, H., Collins, N., Torn, R., and Avellano, A.: The Data Assimilation Research Testbed: A community facility, Bull. Amer. Meteor. Soc., 90, 1283–1296, 2009.

Anderson, J. L.: An Ensemble Adjustment Kalman Filter for Data Assimilation, Mon. Wea. Rev., 129, 2884–2903, 2001.

Anderson, J. L.: An adaptive covariance inflation error correction algorithm for ensemble filters, Tellus, 59A, 210–224, 2007.

Anderson, J. L.: A non-Gaussian ensemble filter update for data assimilation, Mon. Wea. Rev., 138, 4186–4198, 2010.

Anderson, J. L.: A marginal adjustment rank histogram filter for non-Gaussian ensemble data assimilation, Mon. Wea. Rev., 148, 3361–3378, 2020.

Anderson, J. L.: A Quantile-Conserving Ensemble Filter Framework. Part I: Updating an Observed Variable, Mon. Wea. Rev., 150, 1061–1074, 2022.

Barth, A., Canter, M., Van Schaeybroeck, B., Vannitsem, S., Massonnet, F., Zunz, V., Mathiot, P., Alvera-Azcarate, A., and Beckers, J.-M.: Assimilation of sea surface temperature, sea ice concentration and sea ice drift in a model of the Southern Ocean, Ocn. Modelling, 93, 22–39, 2015.

Chen, Z., Liu, J., Song, M., Yang, Q., and Xu, S.: Impacts of assimilating satellite sea ice concentration and thickness on Arctic sea ice prediction in the NCEP Climate Forecast System, J. Climate, 30, 8429–8446, 2017.

Christensen, H., Moroz, I., and Palmer, T.: Simulating weather regimes: Impact of stochastic and perturbed parameter schemes in a simple atmospheric model, Climate Dyn., 44, 2195–2214, 2015.

Chung, E.-S., Ha, K.-J., Timmermann, A., Stuecker, M. F., Bodai, T., and Lee, S.-K.: Cold-season Arctic amplification driven by Arctic ocean-mediated seasonal energy transfer, Earth's Future, 9, e2020EF001 898, 2021.

Danabasoglu, G., Lamarque, J.-F., Bacmeister, J., Bailey, D., DuVivier, A., Edwards, J., Emmons, L., Fasullo, J., Garcia, R., Gettelman, A., et al.: The community earth system model version 2 (CESM2), J. Adv. Mod. Ear. Sys., 12, e2019MS001 916, 2020.

Day, J., Hawkins, E., and Tietsche, S.: Will Arctic sea ice thickness initialization improve seasonal forecast skill?, Geophys. Res. Lett., 41, 7566–7575, 2014.

Dirkson, A., Merryfield, W. J., and Monahan, A.: Impacts of sea ice thickness initialization on seasonal Arctic sea ice predictions, J. Climate, 30, 1001–1017, 2017.

England, M. R., Eisenman, I., Lutsko, N. J., and Wagner, T. J.: The recent emergence of Arctic Amplification, Geophys. Res. Lett., 48, e2021GL094 086, 2021.

Evensen, G.: The ensemble Kalman filter: Theoretical formulation and practical implementation, Ocean dyn., 53, 343–367, 2003.

Fiedler, E. K., Martin, M. J., Blockley, E., Mignac, D., Fournier, N., Ridout, A., Shepherd, A., and Tilling, R.: Assimilation of sea ice thickness derived from CryoSat-2 along-track freeboard measurements into the Met Office's Forecast Ocean Assimilation Model (FOAM), Cryosphere, 16, 61–85, 2022.

Fowler, A. and Jan Van Leeuwen, P.: Observation impact in data assimilation: the effect of non-Gaussian observation error, Tellus A: Dyn. Meteor. Ocn., 65, 20 035, 2013.

Gaspari, G. and Cohn, S. E.: Construction of correlation functions in two and three dimensions, Quart. J. Roy. Meteor. Soc., 125, 723–757, 1999.

Goessling, H. and Jung, T.: A probabilistic verification score for contours: Methodology and application to Arctic ice-edge forecasts, Quart. J. Roy. Meteor. Soc., 144, 735–743, 2018.

https://doi.org/10.5194/egusphere-2023-96
Preprint. Discussion started: 21 March 2023

Goessling, H. F., Tietsche, S., Day, J. J., Hawkins, E., and Jung, T.: Predictability of the Arctic sea ice edge, Geophys. Res. Lett., 43, 1642–1650, 2016.

Hall, D. K., Nghiem, S. V., Rigor, I. G., and Miller, J. A.: Uncertainties of temperature measurements on snow-covered land and sea ice from in situ and MODIS data during BROMEX, J. Climate Appl. Meteor., 54, 966–978, 2015.

Holland, M. M. and Bitz, C. M.: Polar amplification of climate change in coupled models, Climate Dyn., 21, 221–232, 2003.

Holland, M. M., Clemens-Sewall, D., Landrum, L., Light, B., Perovich, D., Polashenski, C., Smith, M., and Webster, M.: The influence of snow on sea ice as assessed from simulations of CESM2, Cryosphere, 15, 4981–4998, 2021.

Houtekamer, P. L. and Zhang, F.: Review of the ensemble Kalman filter for atmospheric data assimilation, Mon. Wea. Rev., 144, 4489–4532, 2016.

Hunke, E. C., Lipscomb, W. H., Turner, A. K., Jeffery, N., and Elliott, S.: CICE: The Los Alamos Sea Ice Model documentation and software user's manual, version 5.1, Los Alamos National Laboratory Doc., LA-CC-06-012, 116, 2015.

Jansen, E., Christensen, J. H., Dokken, T., Nisancioglu, K. H., Vinther, B. M., Capron, E., Guo, C., Jensen, M. F., Langen, P. L., Pedersen, R. A., et al.: Past perspectives on the present era of abrupt Arctic climate change, Nat. Clim. Change, 10, 714–721, 2020.

Jenkins, M. and Dai, A.: The Impact of Sea-Ice Loss on Arctic Climate Feedbacks and Their Role for Arctic Amplification, Geophys. Res. Lett., 48, e2021GL094 599, 2021.

Kalman, R. E.: A new approach to linear filtering and prediction problems, Trans. ASME, 82, 35–45, 1960.

Kimmritz, M., Counillon, F., Bitz, C., Massonnet, F., Bethke, I., and Gao, Y.: Optimising assimilation of sea ice concentration in an Earth system model with a multicategory sea ice model, Tellus: Dyn. Meteor. Ocn., 70, 1–23, 2018.

Kwok, R. and Cunningham, G.: ICESat over Arctic sea ice: Estimation of snow depth and ice thickness, J. Geophys. Res.: Oceans, 113, 2008.

Lawson, W. G. and Hansen, J. A.: Implications of stochastic and deterministic filters as ensemble-based data assimilation methods in varying regimes of error growth, Mon. Wea. Rev., 132, 1966–1981, 2004.

Lei, J., Bickel, P., and Snyder, C.: Comparison of ensemble Kalman filters under non-Gaussianity, Mon. Wea. Rev., 138, 1293–1306, 2010.

Lindsay, R. and Zhang, J.: Assimilation of ice concentration in an ice–ocean model, J. Atmos. Oceanic Technol., 23, 742–749, 2006.

Lipscomb, W. H.: Remapping the thickness distribution in sea ice models, J. Geophys. Res. Oceans, 106, 13 989–14 000, 2001.

Lisæter, K. A., Rosanova, J., and Evensen, G.: Assimilation of ice concentration in a coupled ice–ocean model, using the Ensemble Kalman filter, Ocn. Dyn., 53, 368–388, 2003.

Massonnet, F., Fichefet, T., and Goosse, H.: Prospects for improved seasonal Arctic sea ice predictions from multivariate data assimilation, Ocean Modelling, 88, 16–25, 2015.

Mathiot, P., König Beatty, C., Fichefet, T., Goosse, H., Massonnet, F., and Vancoppenolle, M.: Better constraints on the sea-ice state using global sea-ice data assimilation, Geoscientific Model Development, 5, 1501–1515, 2012.

Meier, W. N. and Maslanik, J. A.: Effect of environmental conditions on observed, modeled, and assimilated sea ice motion errors, J. Geophys. Res.: Oceans, 108, 2003.

Metref, S., Cosme, E., Snyder, C., and Brasseur, P.: A non-Gaussian analysis scheme using rank histograms for ensemble data assimilation, Nonlinear Processes Geophys., 21, 869–885, 2014.

Msadek, R., Vecchi, G. A., Winton, M., and Gudgel, R. G.: Importance of initial conditions in seasonal predictions of Arctic sea ice extent, Geophys. Res. Lett., 41, 5208–5215, 2014.

https://doi.org/10.5194/egusphere-2023-96
Preprint. Discussion started: 21 March 2023

Mu, L., Yang, Q., Losch, M., Losa, S. N., Ricker, R., Nerger, L., and Liang, X.: Improving sea ice thickness estimates by assimilating CryoSat-2 and SMOS sea ice thickness data simultaneously, Quart. J. Roy. Meteor. Soc., 144, 529–538, 2018.

Murphy, J., Sexton, D., Barnett, D., Jones, G., Webb, M., Collins, M., and Stainforth, D.: Quantifying uncertainties in climate change from a large ensemble of general circulation model predictions, Nature, 430, 768–772, 2004.

Orth, R., Dutra, E., and Pappenberger, F.: Improving weather predictability by including land surface model parameter uncertainty, Mon. Wea. Rev., 144, 1551–1569, 2016.

Pham, D. T.: Stochastic methods for sequential data assimilation in strongly nonlinear systems, Mon. Wea. Rev., 129, 1194–1207, 2001.

Pires, C. A., Talagrand, O., and Bocquet, M.: Diagnosis and impacts of non-Gaussianity of innovations in data assimilation, Physica D: Nonlin. Phenon., 239, 1701–1717, 2010.

Raeder, K., Hoar, T. J., El Gharamti, M., Johnson, B. K., Collins, N., Anderson, J. L., Steward, J., and Coady, M.: A new CAM6+DART reanalysis with surface forcing from CAM6 to other CESM models, Scientific Reports, 11, 1–24, 2021.

Rantanen, M., Karpechko, A. Y., Lipponen, A., Nordling, K., Hyvärinen, O., Ruosteenoja, K., Vihma, T., and Laaksonen, A.: The Arctic has warmed nearly four times faster than the globe since 1979, Communications Earth & Environment, 3, 1–10, 2022.

Ricker, R., Hendricks, S., Kaleschke, L., Tian-Kunze, X., King, J., and Haas, C.: A weekly Arctic sea-ice thickness data record from merged CryoSat-2 and SMOS satellite data, Cryosphere, 11, 1607–1623, 2017.

Rostosky, P., Spreen, G., Gerland, S., Huntemann, M., and Mech, M.: Modeling the microwave emission of snow on Arctic sea ice for estimating the uncertainty of satellite retrievals, J. Geophys. Res. Oceans, 125, e2019JC015 465, 2020.

Sakov, P., Counillon, F., Bertino, L., Lisæter, K., Oke, P., and Korablev, A.: TOPAZ4: an ocean-sea ice data assimilation system for the North Atlantic and Arctic, Ocn. Science, 8, 633–656, 2012a.

Sakov, P., Oliver, D. S., and Bertino, L.: An iterative EnKF for strongly nonlinear systems, Mon. Wea. Rev., 140, 1988–2004, 2012b.

Screen, J. A. and Simmonds, I.: The central role of diminishing sea ice in recent Arctic temperature amplification, Nature, 464, 1334–1337, 2010.

Serreze, M., Barrett, A., Stroeve, J., Kindig, D., and Holland, M.: The emergence of surface-based Arctic amplification, Cryosphere, 3, 11–19, 2009.

Serreze, M. C. and Francis, J. A.: The Arctic amplification debate, Climate Change, 76, 241–264, 2006.

Stainforth, D. A., Aina, T., Christensen, C., Collins, M., Faull, N., Frame, D. J., Kettleborough, J. A., Knight, S., Martin, A., Murphy, J., et al.: Uncertainty in predictions of the climate response to rising levels of greenhouse gases, Nature, 433, 403–406, 2005.

Stark, J. D., Ridley, J., Martin, M., and Hines, A.: Sea ice concentration and motion assimilation in a sea ice- ocean model, J. Geophys. Res.: Oceans, 113, 2008.

Tietsche, S., Day, J. J., Guemas, V., Hurlin, W., Keeley, S., Matei, D., Msadek, R., Collins, M., and Hawkins, E.: Seasonal to interannual Arctic sea ice predictability in current global climate models, Geophys. Res. Lett., 41, 1035–1043, 2014.

Tilling, R. L., Ridout, A., and Shepherd, A.: Near-real-time Arctic sea ice thickness and volume from CryoSat-2, Cryosphere, 10, 2003–2012, 2016.

Tippett, M. K., Anderson, J. L., Bishop, C. H., Hamill, T. M., and Whitaker, J. S.: Ensemble Square Root Filters, Mon. Wea. Rev., 131, 2003.

Urrego-Blanco, J. R., Urban, N. M., Hunke, E. C., Turner, A. K., and Jeffery, N.: Uncertainty quantification and global sensitivity analysis of the Los Alamos sea ice model, J. Geophys. Res. Oceans, 121, 2709–2732, 2016.

Van Woert, M. L., Zou, C.-Z., Meier, W. N., Hovey, P. D., Preller, R. H., and Posey, P. G.: Forecast verification of the Polar Ice Prediction System (PIPS) sea ice concentration fields, Journal Atmos. Ocn. Tech., 21, 944–957, 2004.

https://doi.org/10.5194/egusphere-2023-96
Preprint. Discussion started: 21 March 2023

Walsh, J. E.: Intensified warming of the Arctic: Causes and impacts on middle latitudes, Glob. Planet. Change, 117, 52–63, 2014.

Welch, B. L.: The generalization of 'STUDENT'S' problem when several different population variances are involved, Biometrika, 34, 28–35, 1947.

Yu, L., Zhong, S., Vihma, T., and Sun, B.: Attribution of late summer early autumn Arctic sea ice decline in recent decades, npj Clim. and Atmos. Sci., 4, 1–14, 2021.

Zampieri, L., Goessling, H. F., and Jung, T.: Bright prospects for Arctic sea ice prediction on subseasonal time scales, Geophys. Res. Lett., 45, 9731–9738, 2018.

Zhang, Y.-F., Bitz, C. M., Anderson, J. L., Collins, N., Hendricks, J., Hoar, T., Raeder, K., and Massonnet, F.: Insights on sea ice data assimilation from perfect model observing system simulation experiments, J. Climate, 31, 5911–5926, 2018.

https://doi.org/10.5194/egusphere-2023-96
Preprint. Discussion started: 21 March 2023

Table 1. List of CICE-DART OSSEs with the different configurations.

Experiments	Assimilated Observations	Modified Forward Operator	Postprocessed States	Assimilation Algorithm	State Vector
Exp. 1	SIC,SIT	No	VSNON	EAKF	AICEN,VICEN
Exp. 2	SIC,SIT,SNWD	No	—	EAKF	AICEN,VICEN,VSNON
Exp. 3	SIT,SNWD	No	—	EAKF	AICEN,VICEN,VSNON
Exp. 4	SIC,SIT,SNWD	No	—	RHF	AICEN,VICEN,VSNON
Exp. 5	SIT,SNWD	Yes	—	EAKF	AICEN,VICEN,VSNON
Exp. 6	SIT,SNWD,SIST	Yes	—	EAKF	AICEN,VICEN,VSNON

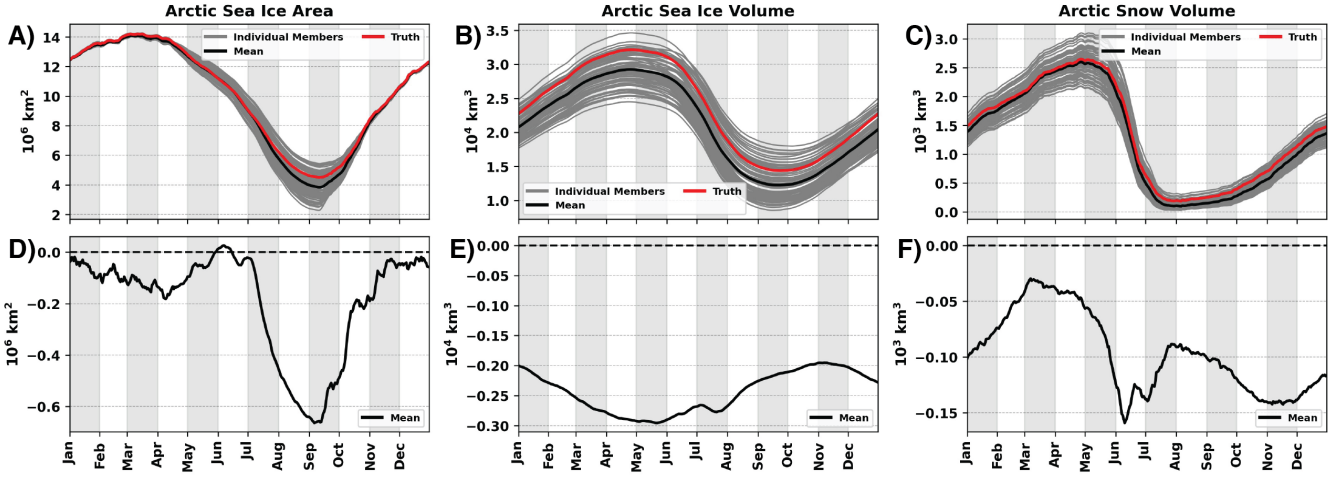

Figure 1. Daily total Arctic (A) sea ice area, (B) sea ice volume, and (C) snow volume from CICE5 free forecast simulations. Each gray line represents an individual ensemble member, black line represents the ensemble mean, and the red line represents the truth member. The truth member is a randomly selected ensemble member. Daily biases of the total Arctic (A) sea ice area, (B) sea ice volume, and (C) snow volume where the black line represents the ensemble mean difference compared to the truth. The black dashed line is the zero reference line. The free forecast period is for the year 2013.

https://doi.org/10.5194/egusphere-2023-96
Preprint. Discussion started: 21 March 2023

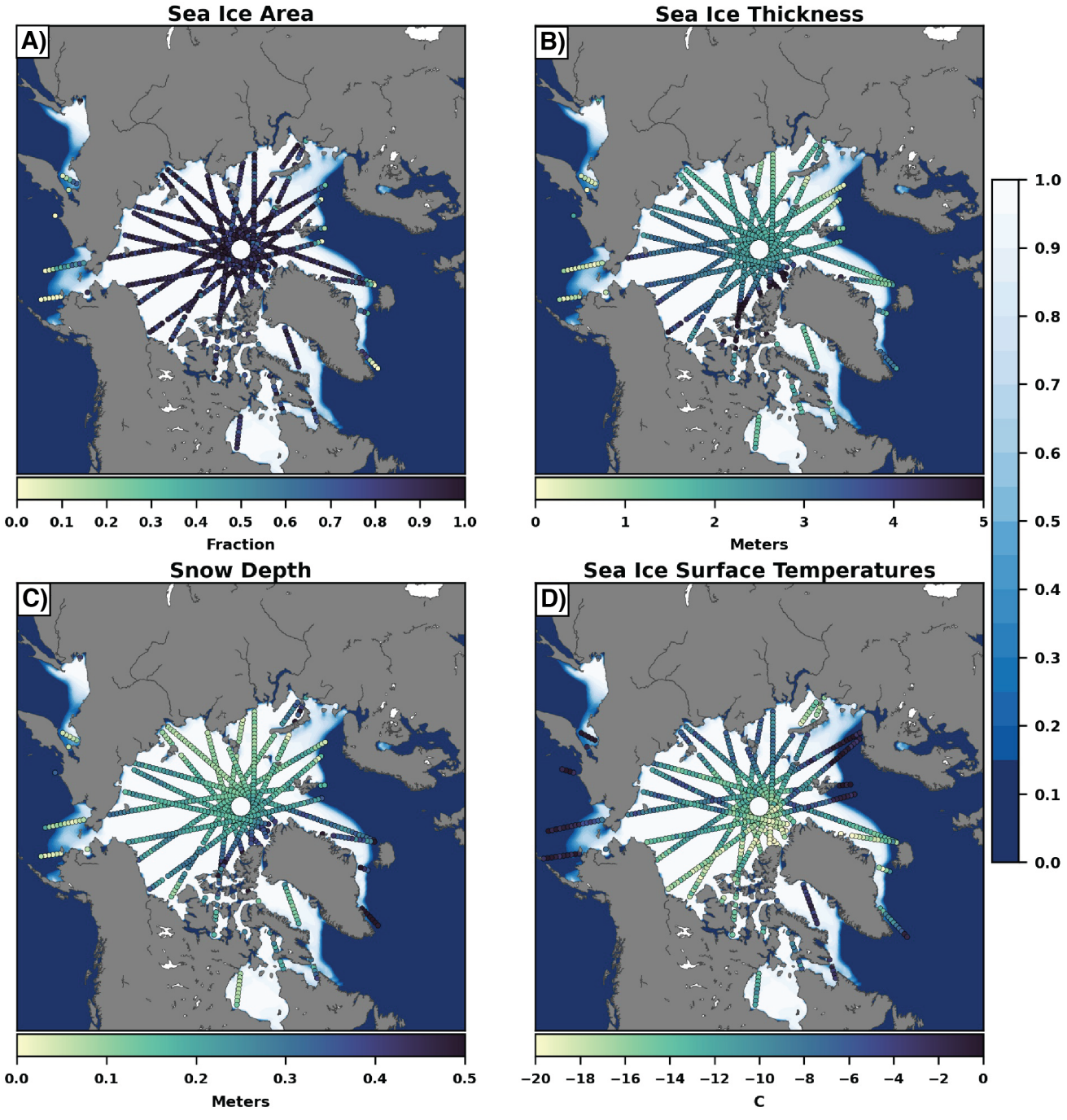

Figure 2. An example of the spatial locations of assimilated (A) sea ice area, (B) sea ice thickness,(C) snow depth and (D) sea ice surface temperature observations. Colorfill is the ensemble mean of the sea ice area and the dots are the observation locations along with their associated value.

https://doi.org/10.5194/egusphere-2023-96
Preprint. Discussion started: 21 March 2023

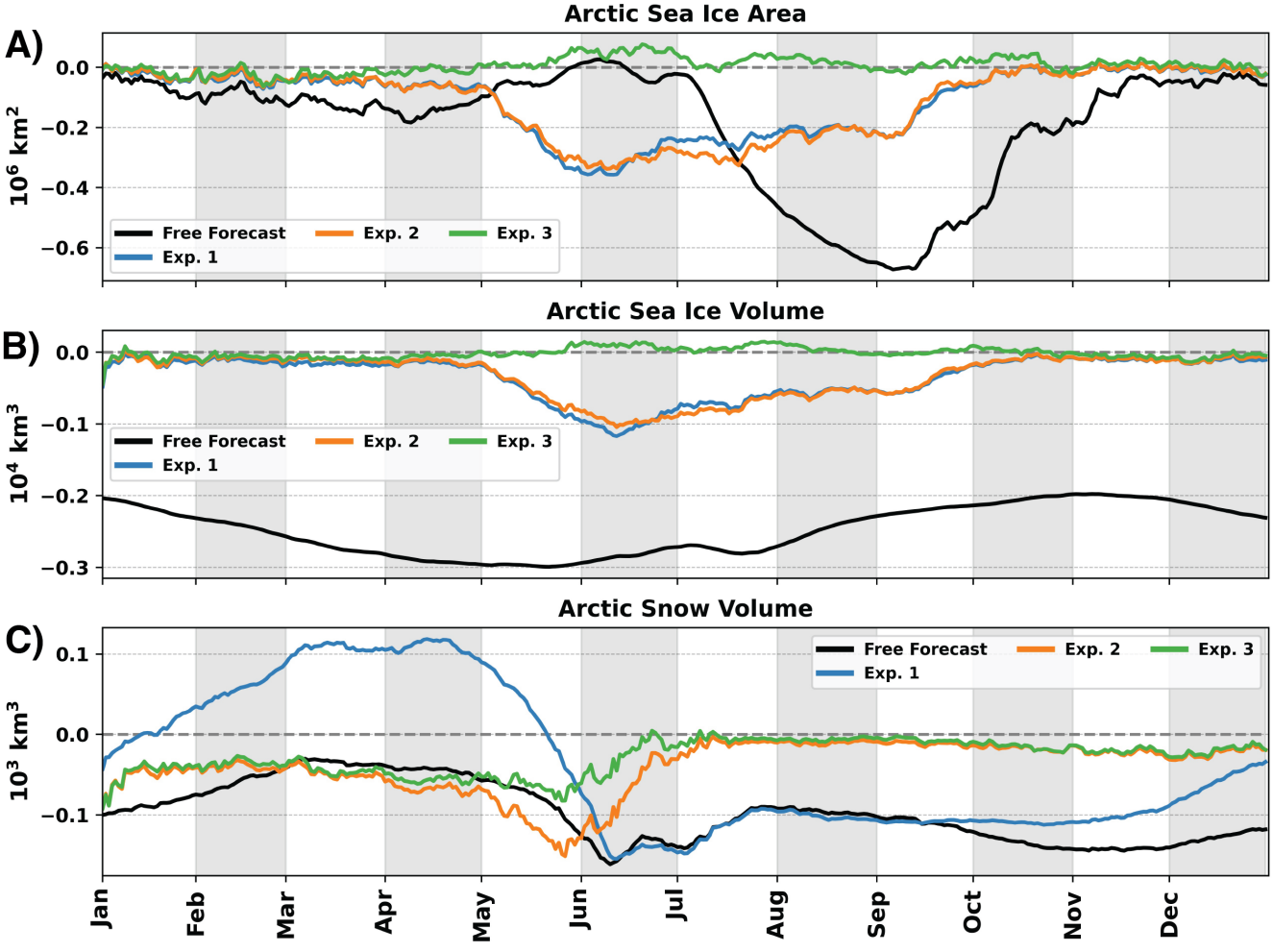

Figure 3. Daily biases of the Arctic total (A) sea ice area, (B) sea ice volume, and (C) snow volume from the free forecasts and experiments 1–3. Gray dashed lines are the zero reference line.

https://doi.org/10.5194/egusphere-2023-96
Preprint. Discussion started: 21 March 2023

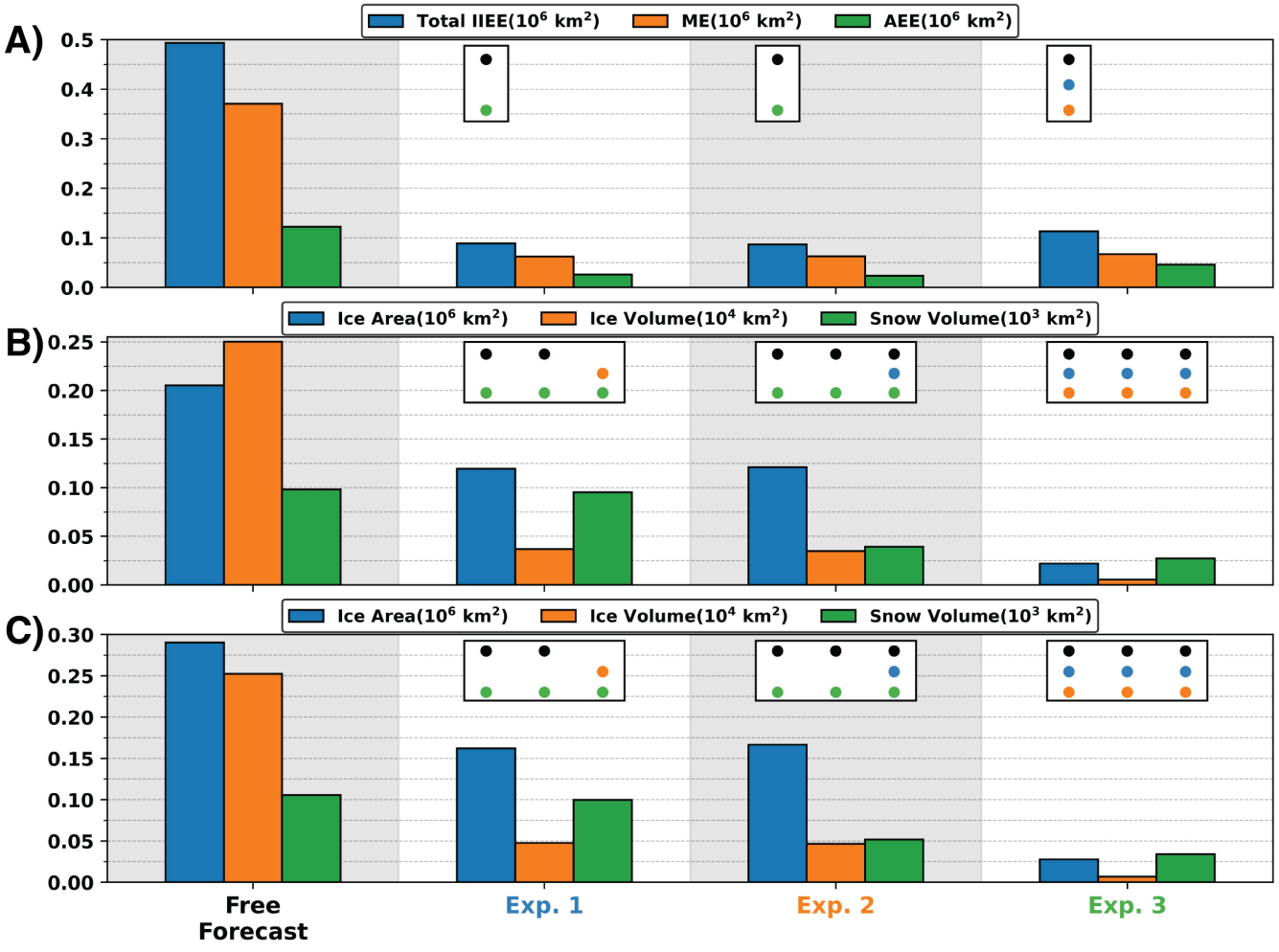

Figure 4. The (A) IIEE, (B) MAB, and (C) RMSE of sea ice area, sea ice volume and snow volume from the free forecast and experiments 1–3. Each index is computed using the ensemble mean and over the entire cycling period. Dots represents an pairs of experiments that are significantly different from a different experiment using a student t-test. Dot colors correspond to the different experiments.

https://doi.org/10.5194/egusphere-2023-96
Preprint. Discussion started: 21 March 2023

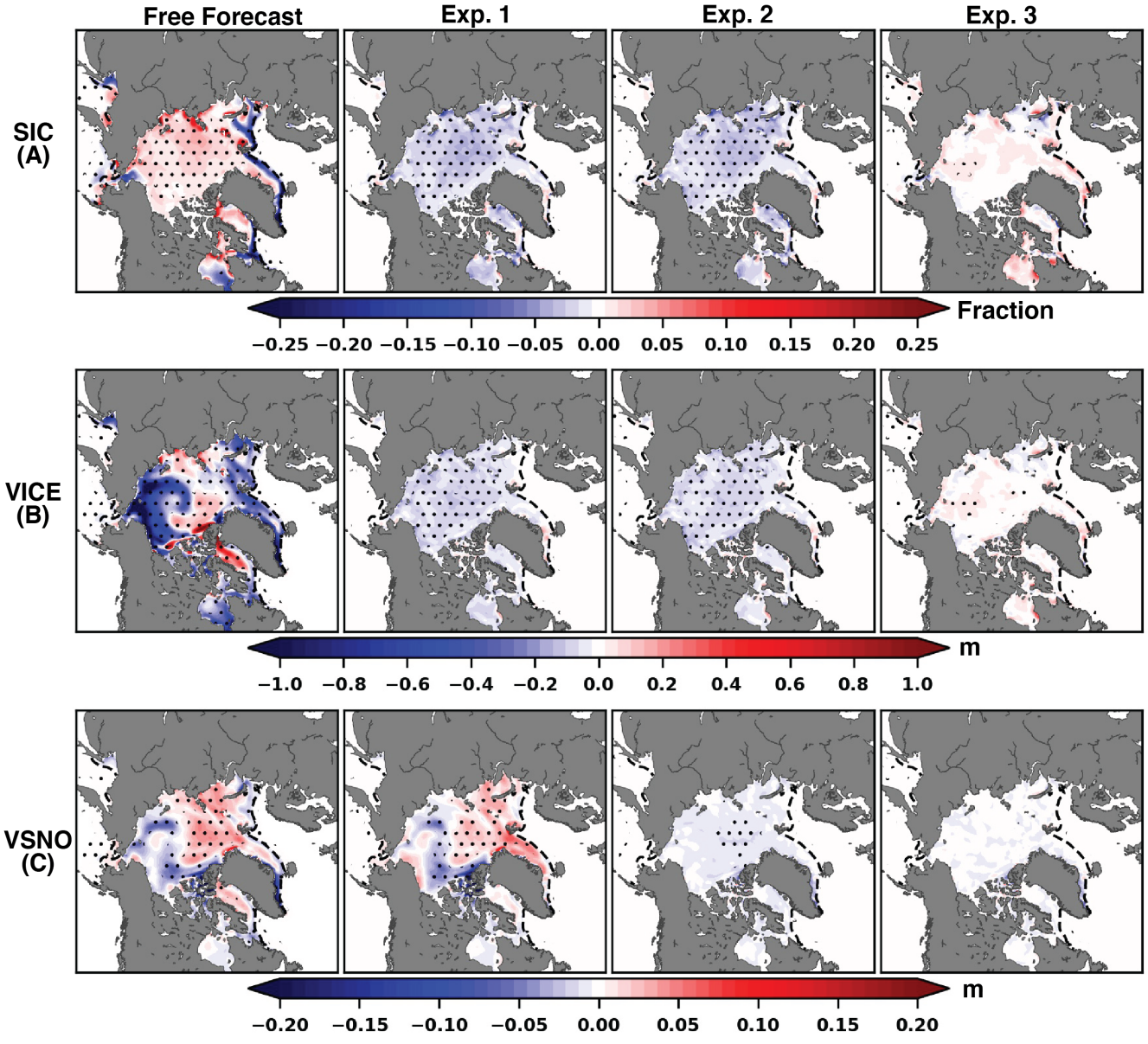

Figure 5. Ensemble mean spatial biases of (A) SIC, (B) VICE, and (C) VSNO averaged over May–June for the free forecast and experiments 1–3. Stippling represents significant biases at the 95% confidence interval using a Welch's t-test. The black dashed line is the sea ice edge (0.15 SIC).

https://doi.org/10.5194/egusphere-2023-96
Preprint. Discussion started: 21 March 2023

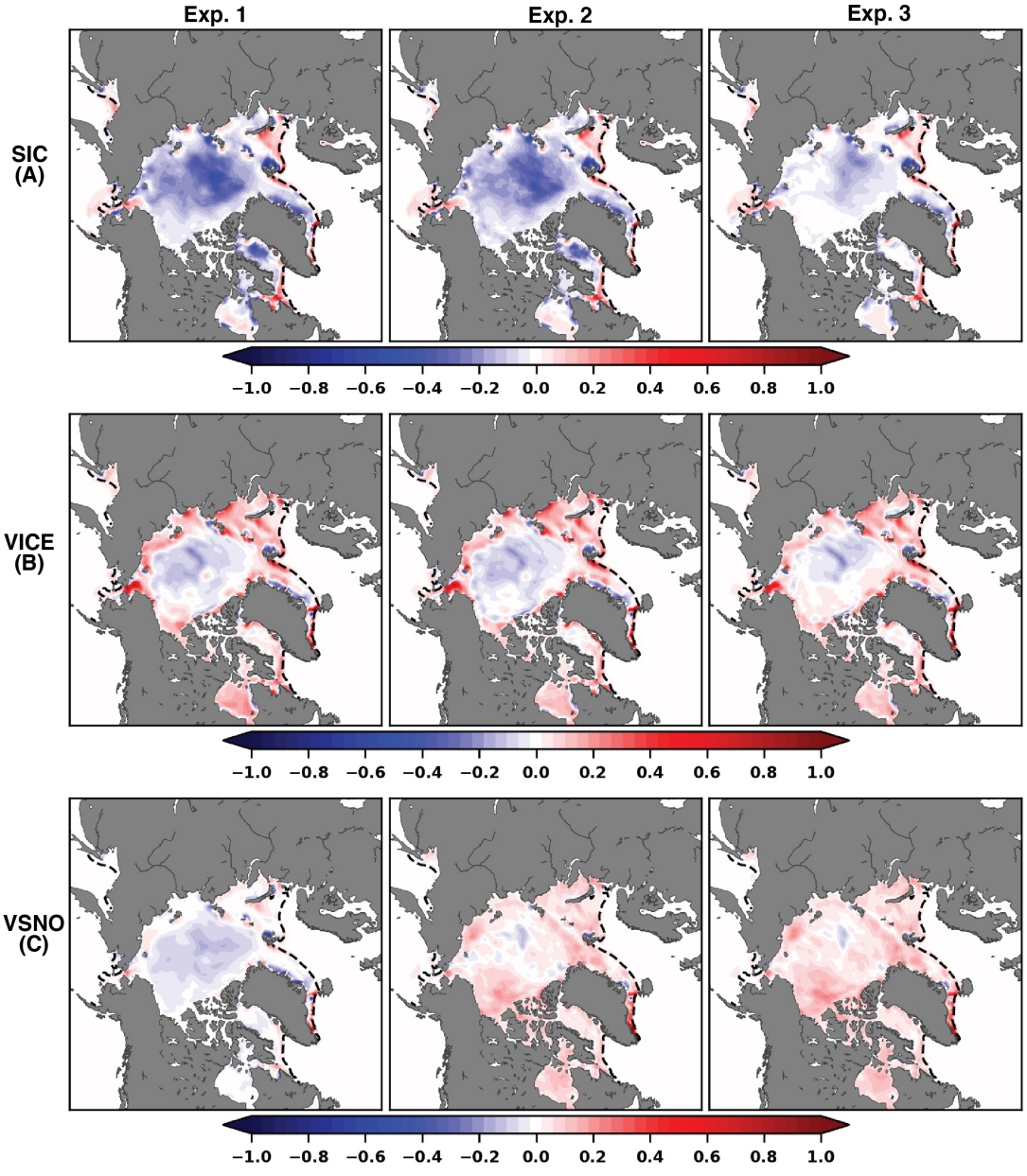

Figure 6. Normalized spatial analysis increments of (A) SIC, (B) VICE, and (C) VSNO averaged over May–June for experiments 1–3. Analysis increments of SIC, VICE, and VSNO were normalized using the largest absolute value from across the three experiments. The black dashed line is the sea ice edge (0.15 SIC).

https://doi.org/10.5194/egusphere-2023-96
Preprint. Discussion started: 21 March 2023

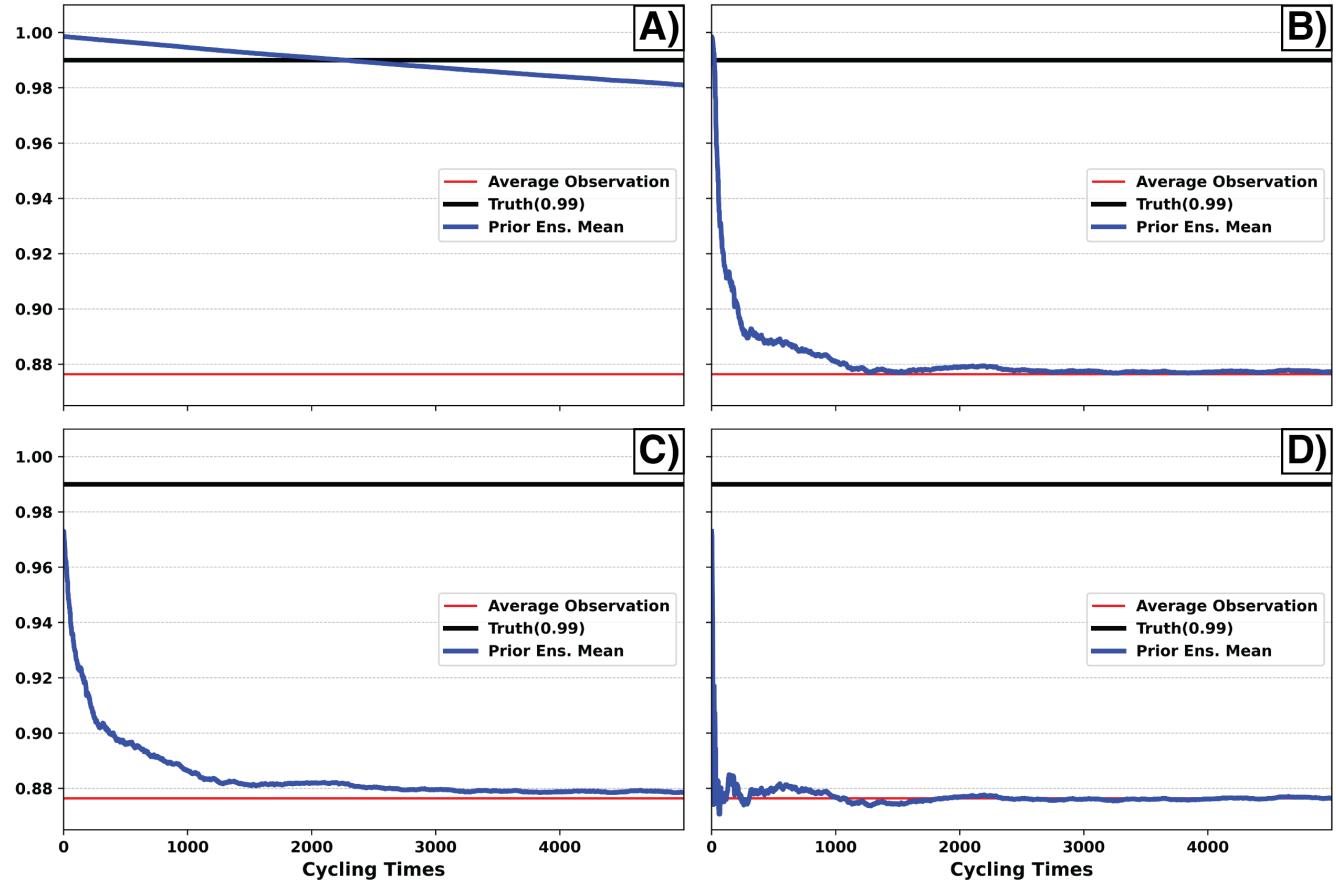

Figure 7. Prior ensemble mean (blue line) time series of SIC for experiments using (A,B) small initial ensemble spread and (C,D) large initial ensemble spread. Each experiment was completed with prior inflation (A,C) turned off and (B,D) turned on. The red line represents the average observation value over the cycling period. The black line represents the true value over the cycling period.

https://doi.org/10.5194/egusphere-2023-96
Preprint. Discussion started: 21 March 2023

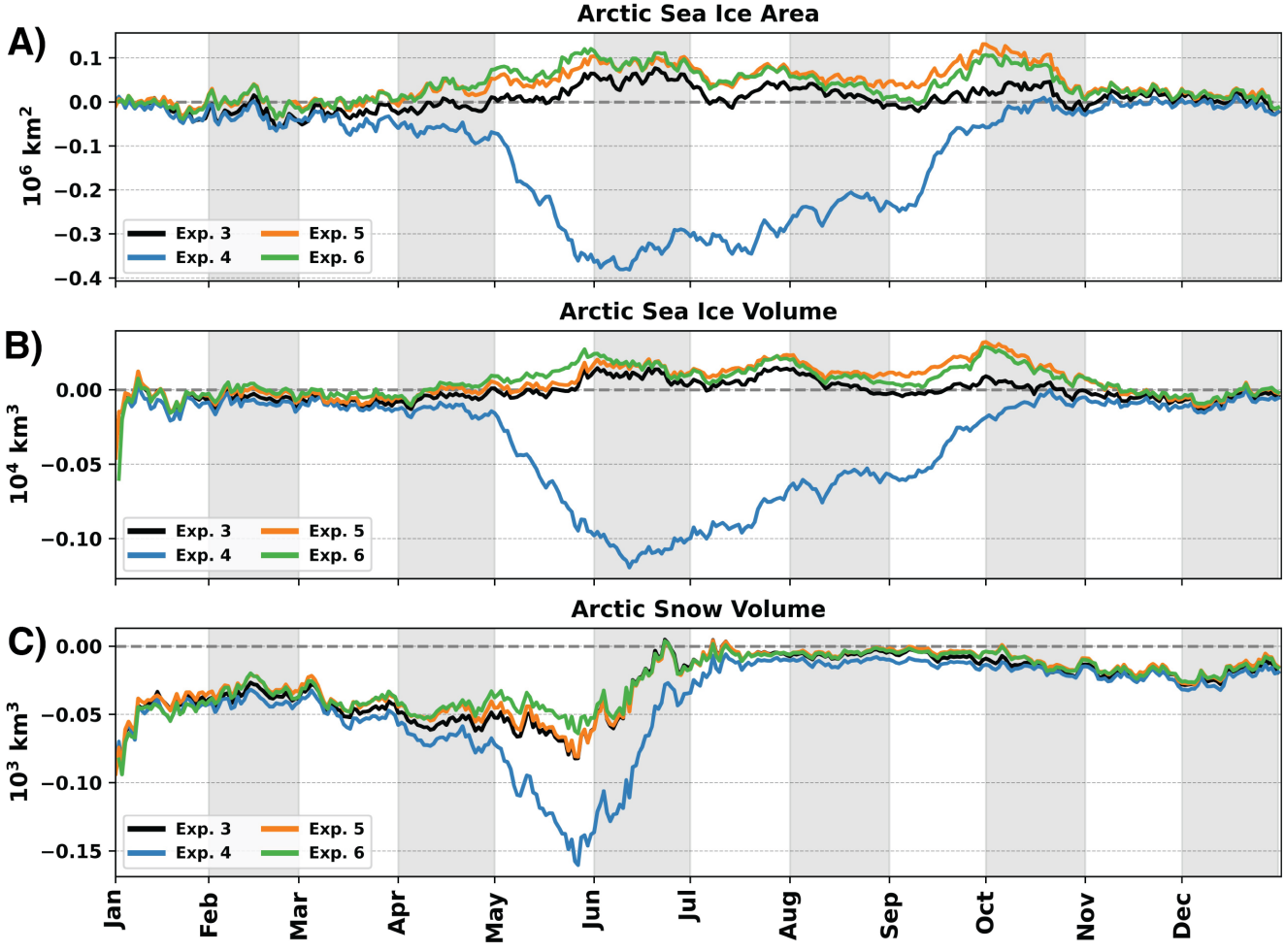

Figure 8. Same as Figure 3 but for experiments 3–6.

https://doi.org/10.5194/egusphere-2023-96
Preprint. Discussion started: 21 March 2023

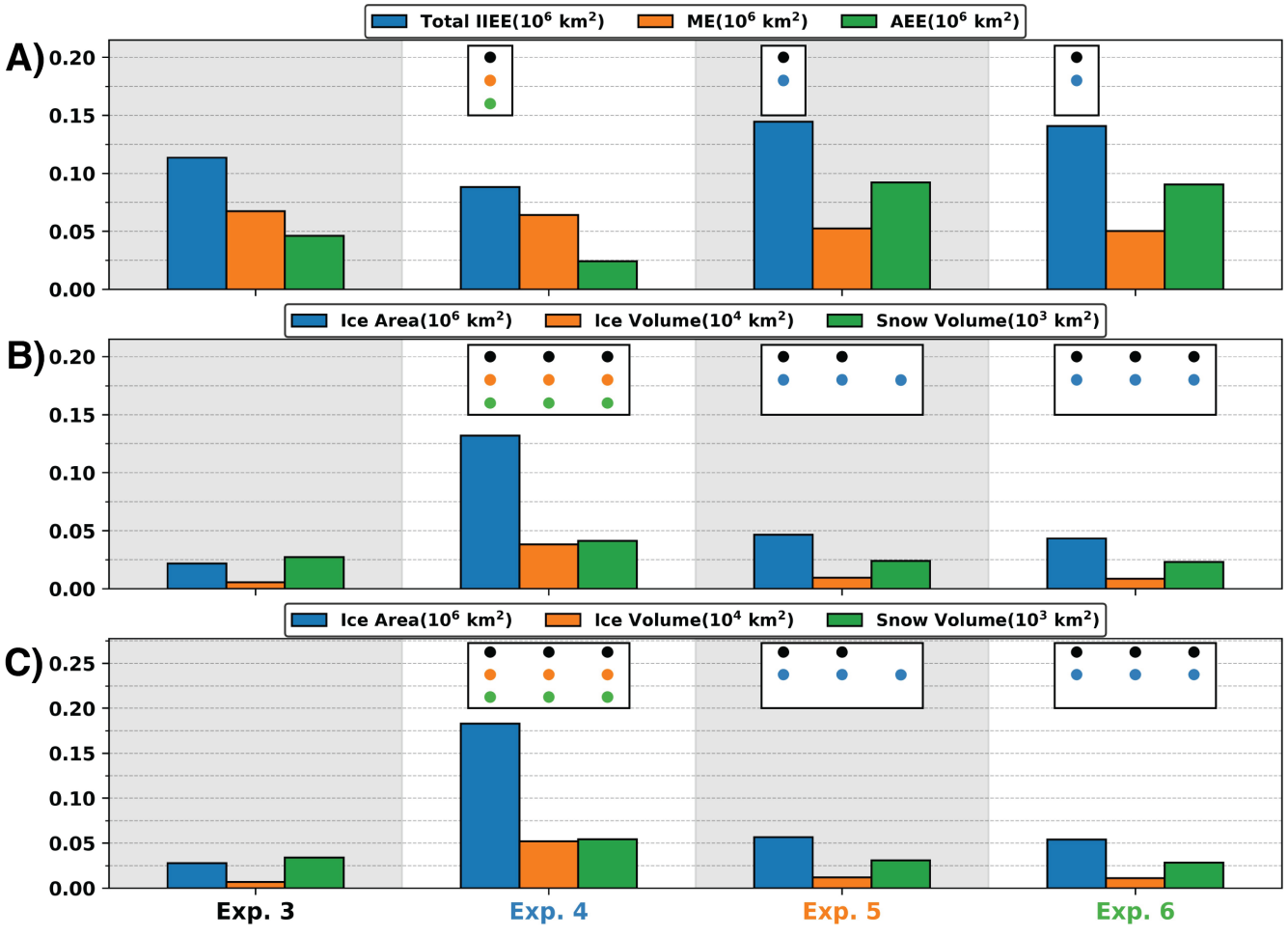

Figure 9. Same as Figure 4 but for experiments 3–6.

https://doi.org/10.5194/egusphere-2023-96
Preprint. Discussion started: 21 March 2023

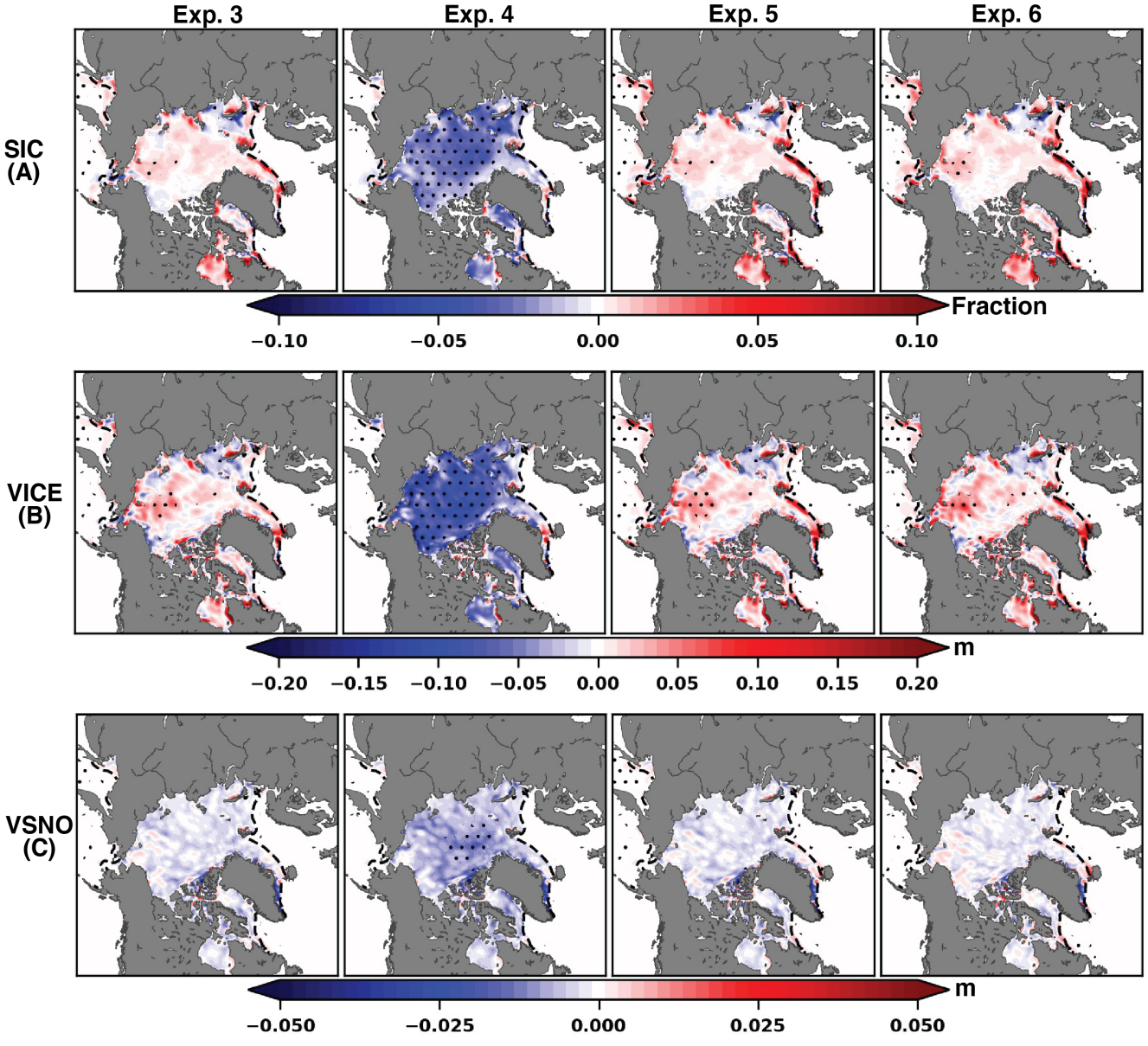

Figure 10. Same as Figure 5 but for experiments 3–6.

https://doi.org/10.5194/egusphere-2023-96
Preprint. Discussion started: 21 March 2023

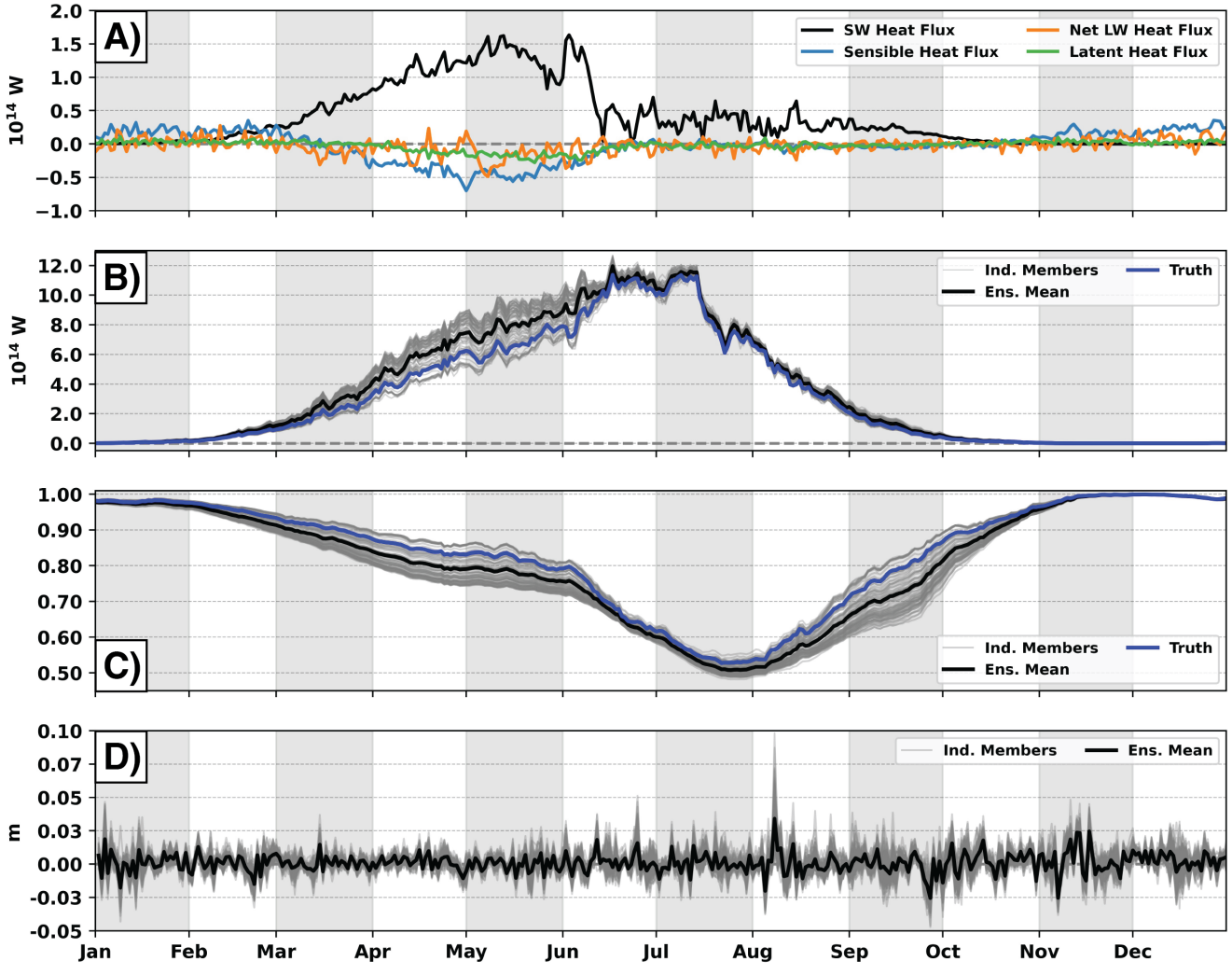

Figure 11. Panel (A): Ensemble mean daily biases of sea ice accumulated atmospheric heat fluxes for experiment 3 compared to the truth. The plotted atmospheric heat flux components include: shortwave heat flux (black line), sensible heat flux (blue line), net longwave heat flux (orange line), and latent heat flux (green line). Gray dashed line represents the zero reference line. **Panel (B):** Time series of sea ice accumulated shortwave heat flux for experiment 3. The gray lines are the individual ensemble members, the black line is the ensemble mean, and the blue line is the truth. Gray dashed line represents the zero reference line. **Panel (C):** Same as Panel (B) but for mean surface albedo over sea ice. **Panel (D):** Daily biases of sea ice accumulated snowfall for experiment 3 compared to the truth. The gray lines are the individual ensemble members, and the black line is the ensemble mean.

https://doi.org/10.5194/egusphere-2023-96
Preprint. Discussion started: 21 March 2023

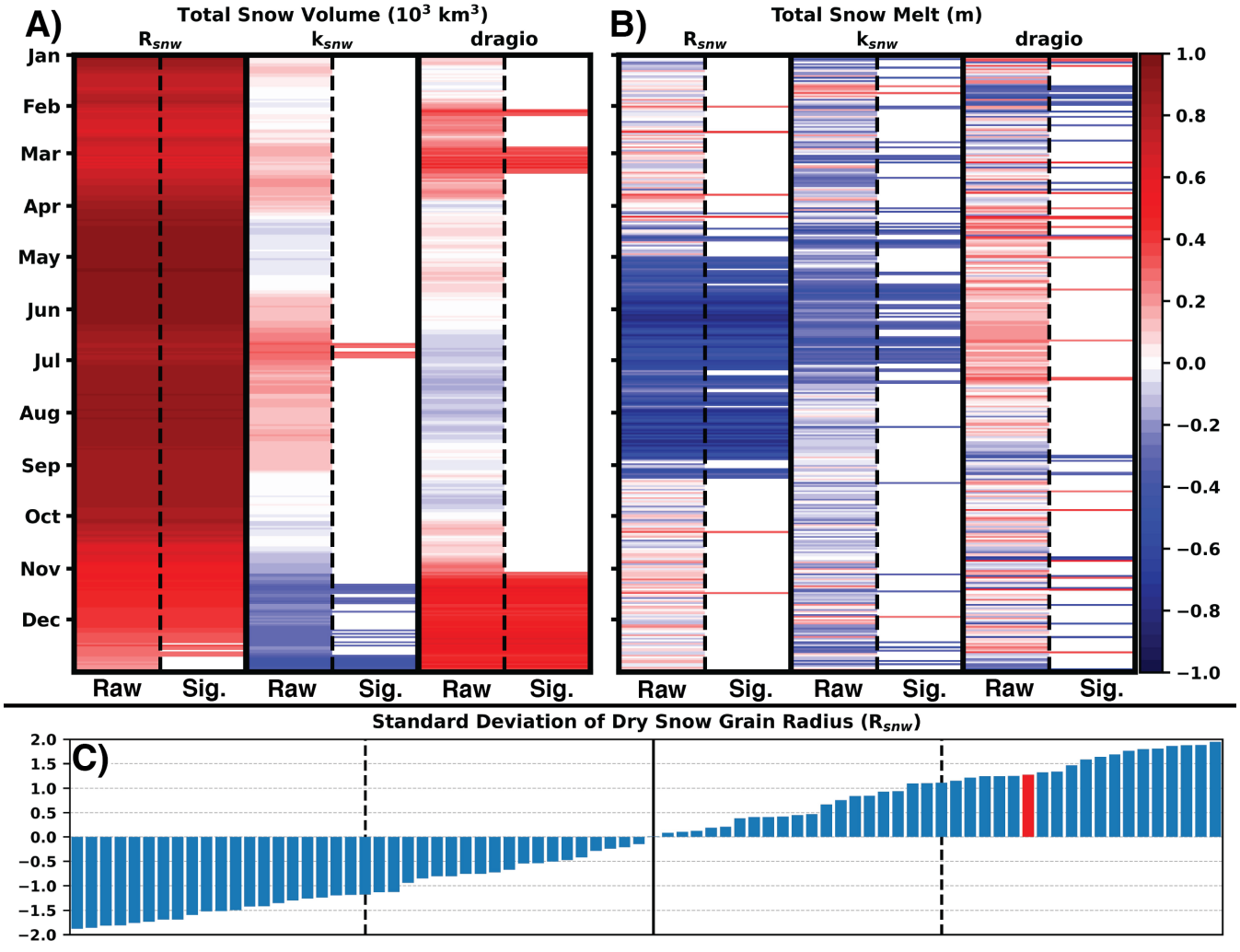

Figure 12. Panel (A): Daily correlations between perturbed CICE parameters and total snow volume over the Arctic. Correlations are computed using a Spearman's rank correlation method where both the raw correlations (**Raw**) and significant correlations with confidence at 99% (**Sig.**) are shown. **Panel (B):** Same as Panel (A) but for total snow melt over the sea ice in the Arctic. **Panel (C):** Sorted perturbed R_{snw} parameter values for each ensemble member. Red bar indicates the truth member. Black line is the median and the two dash lines represent the interquartile range.